



Effect of Design Parameters on Tension Clip Strength

Seif Elbadry, Mahmoud Tash, Mostafa Shazly

Student, Mechanical Engineering Department, Faculty of Engineering, The British University in Egypt - Cairo, Egypt

Full Professor, Mechanical Engineering Department, Faculty of Engineering, The British University in Egypt - Cairo, Egypt

Full Professor, Mining, Petroleum and Metallurgical Engineering Department, The British University in Egypt - Cairo, Egypt

ABSTRACT: Polymer matrix composite introduction to the Science of Materials was revolutionary to the industrial sector. It is used in wide range of applications due to its mechanical properties, such as infrastructure, marine, automotive, and aerospace. This paper aims to investigate the effects of stacking orientation and hole clearance around the bolt on the failure of the L-joint. It was found out that the stacking orientation ($0^\circ, 45^\circ, -45^\circ$) and larger hole clearance increase the strength of the L-joint. Changing the hole clearance and stack orientation had major influence on the strength of the bolted joint and the behaviour of material failure.

KEYWORDS: Bolted Joints; L-Joint; Glass Fiber Reinforced Plastic (GFRP); Finite Element Analysis (FEA)

I. INTRODUCTION

The introduction of polymer matrix composites (PMCs) to materials science and industry was milestone that integrated higher material mechanical properties in terms of high strength and stiffness to weight ratio, resistance to corrosion, etc. with a sustainable solution that is friendly to the environment and can be used in many industries and applications such as cities infrastructure, marine, automotive and aerospace (1,2).

Bolted joints are used to connect structures mechanically in a wide range of applications such as aircraft, civil steel and concrete structures, and defense projects (3-7). Bolted joints can be one of two types, depending on acting forces relative to the joint: tensile if the forces are parallel to the axis, and shear if the forces are perpendicular, both of which are presented in Figure 1. Bolted joint connections offer some advantages over other connection methods, such as adhesive joints, including ease of assembly and dismantling, and resistance to chemically induced degradation. [8,9]

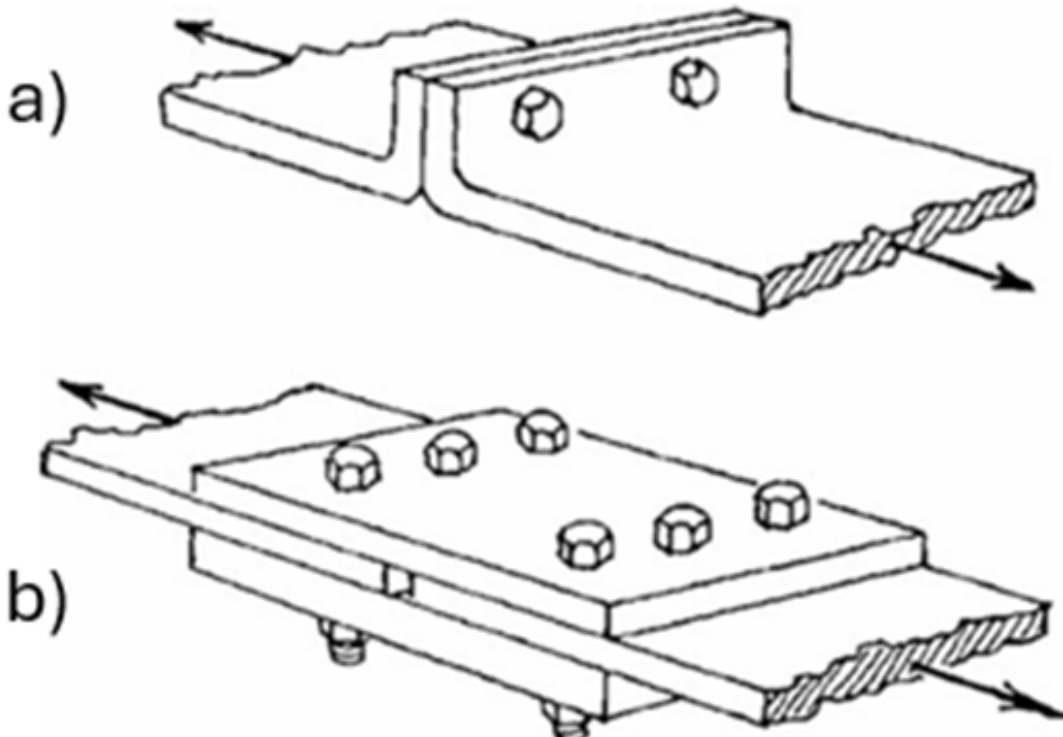


Figure 1: a) Tensile loading. b) Shear loading [8]

Bolted joints can fail in many ways, such as the bolt loosening, breaking, corroding, cracking, or becoming fatigued. Most of these failures happen when the bolt does not have enough preload, meaning the clamping force holding the joint together is too low. When the clamping force is too small, the parts of the joint can start to slip back and forth during vibration, which leads to several problems: the bolt loosens, the joint becomes misaligned, surfaces rub and corrode, and the load is carried in the wrong way, which causes fatigue damage. This is especially dangerous in shear joints, where sideways forces are supported by friction. In tensile joints, a low clamp can let the joint parts separate. When this happens, the bolt loses all clamping force, which can lead to fatigue, weaken the structure, and expose the joint to corrosion [8].

There is a total of 6 possible failure modes, which can be described as follows and illustrated in Figure 2, namely, bearing failure, net-tension failure, shear-out failure, cleavage failure, fastener pull-through, and bolt failure.

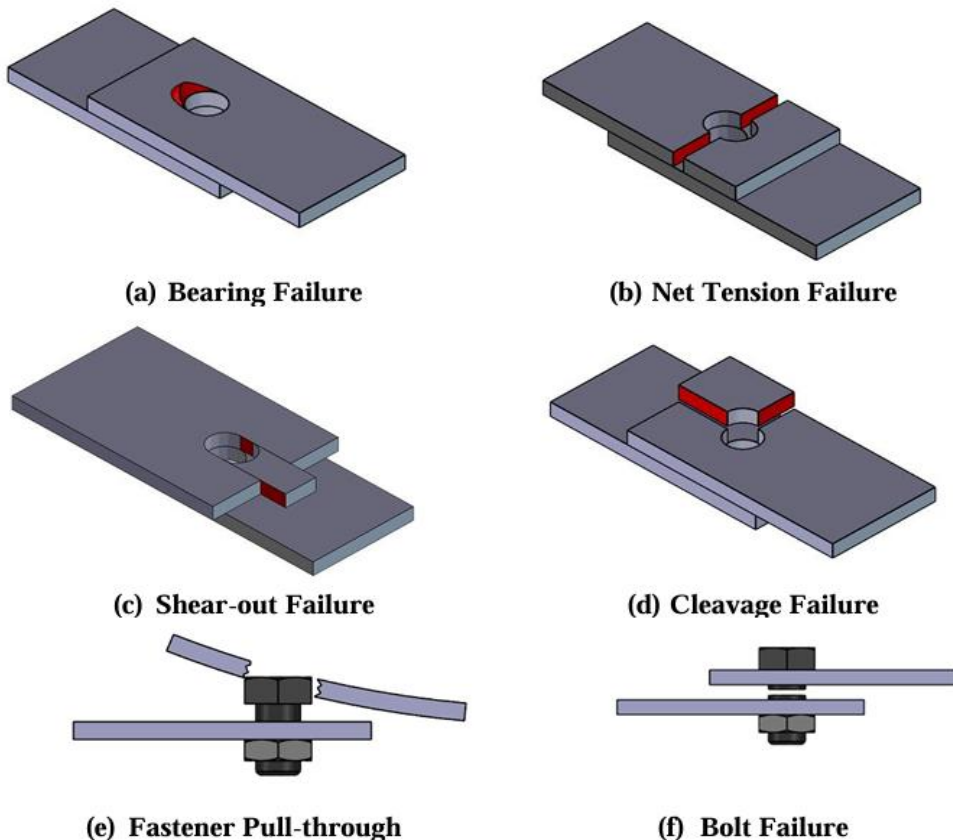


Figure 2: Different Failure Modes [10]

Poor structural design can lead to the first five failure modes, while the last results from overloading. Bearing failure is preferred because it progresses gradually and provides warning signs, whereas the other modes occur suddenly and can be catastrophic to the entire structure [10,11]. This work continues the investigation into failure modes resulting from tensile loading done by Hassan et al. [10], by further testing the effect of variables on the mechanical properties of the bolted joint.

II. RESEARCH METHOD

A. MODEL DESCRIPTION

L-shaped samples were developed to simulate the process of tensile testing on ABAQUS Simulia2024®/Standard solver. The model composite layer is built layer by layer, and the components are bolts, nuts, washers, and L-joint triaxial layer as shown in Figures 3 and 4. All parts are modeled as deformable particles. The materials used for this research are GFRP/Epoxy for the L-joints, and its mechanical properties are listed below in Table 1.

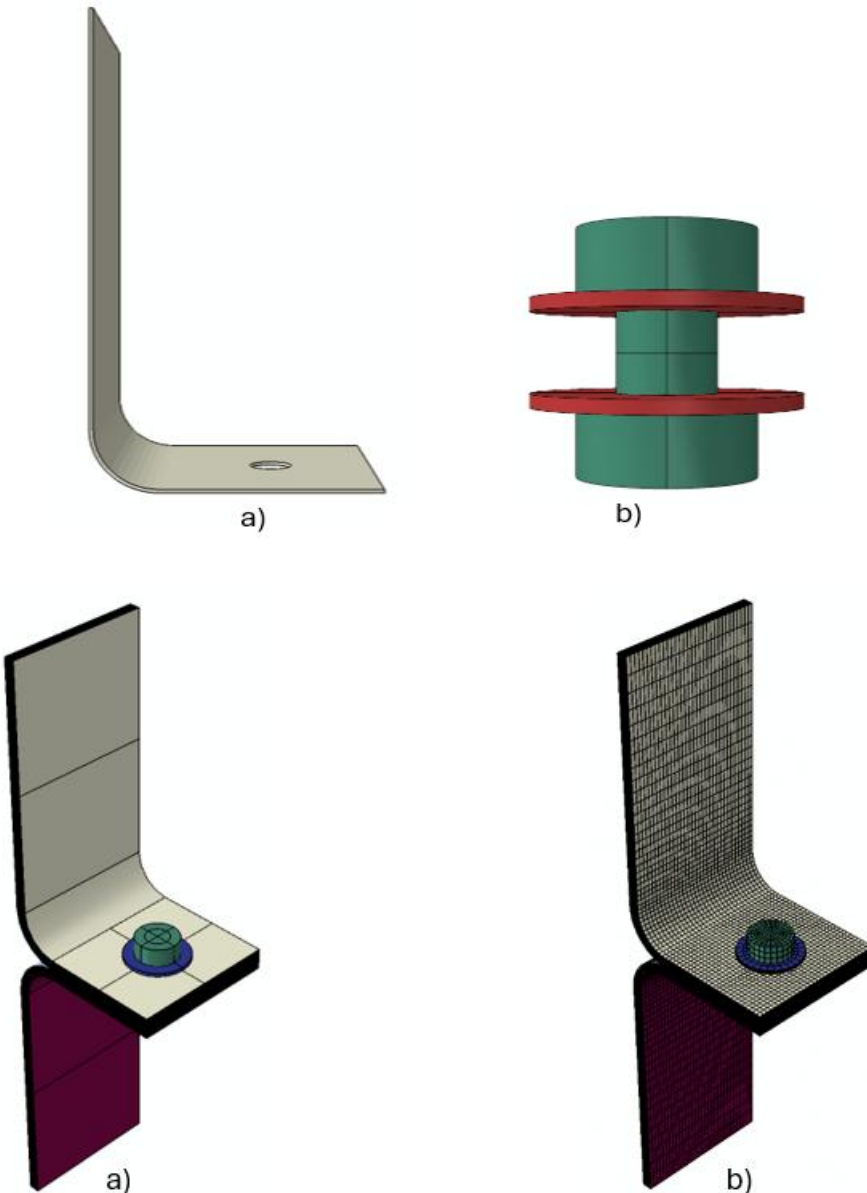
Table 1 GFRP/Epoxy mechanical properties

Property	Value
Density (kg/m ³)	1888.1
E ₁₁ (GPa)	44.25
E ₂₂ = E ₃₃ (GPa)	10.95
V ₁₂ = V ₁₃	0.236
V ₂₃	0.368
G ₁₂ = G ₁₃ (GPa)	4.6
G ₂₃ (GPa)	4

The variables considered were hole clearance (%) and ply orientation. A total of 6 models were generated, each unique with different combinations of these variables listed in table 2. This approach allowed for a systematic investigation of how each variable, individually and in combination with others, influences structural behavior.

Table 2: List of Models

Run	Hole Clearance (%)	Number of Plies	Stacking Sequence
1	5%	5	(0°, 45°, -45°)
2	10%	5	(0°, 45°, -45°)
3	15%	5	(0°, 45°, -45°)
4	5%	5	(90°, 45°, -45°)
5	10%	5	(90°, 45°, -45°)
6	15%	5	(90°, 45°, -45°)





B. MESHING, BOUNDARY CONDITIONS AND CONTACT BEHAVIOR

Similar parameters were used to the investigation carried out by Hassan et al [10] with some adjustments to the meshing and loading. The joint is loaded with 40 mm in the vertical direction while being fixed from the opposite end. ABAQUS standard is used to simulate the preload, and ABAQUS Explicit uses the output from the standard as a predefined field.

Surface-to-surface contact was used to define the contact surface between the different parts of the model. Meshing was concentrated on the L-joint, specifically in the curved areas, while it was reduced on the washer and bolt as shown in Figure 4b). ABAQUS defines the damage criteria using Hashin and Rotem criteria, which could be broken down to four main mechanisms [12,13]: Fiber compression, Fiber tension, Matrix compression, and Matrix tension.

Those mechanisms can be defined using the equations below. Where σ_{11} , σ_{22} and σ_{12} represents the stress components applied while the coefficient α is the factor that determines how much shear stress contributes to the fiber direction.

Fiber tension ($\sigma_{11} \geq 0$)

$$F_f^t = \left(\frac{\sigma_{11}}{X^T} \right)^2 + \alpha \left(\frac{\sigma_{12}}{S_{12}} \right)^2$$

Fiber compression ($\sigma_{11} < 0$)

$$F_f^c = \left(\frac{\sigma_{11}}{X^C} \right)^2$$

Matrix tension ($\sigma_{22} \geq 0$)

$$F_m^t = \left(\frac{\sigma_{22}}{Y^T} \right)^2 + \left(\frac{\sigma_{12}}{S_{12}} \right)^2$$

Matrix compression ($\sigma_{22} < 0$)

$$F_m^c = \left(\frac{\sigma_{22}}{2S_{23}} \right)^2 + \left[\left(\frac{Y^C}{2S_{23}} \right)^2 - 1 \right] \frac{\sigma_{22}}{Y^C} + \left(\frac{\sigma_{12}}{2S_{12}} \right)^2$$

III. TESTS RESULTS

A. VARIABLE EFFECTS ON STRENGTH

Observing Figures 5 and 6, it is shown that the model experiences the longest duration of elastic deformation when the hole clearance is 10%, while at 15% the model experiences the highest loads. Also, when comparing stacking orientation, models with (90°, 45°, -45°) experience longer elastic deformation than those with (0°, 45°, -45°), they can withstand less load. Table 3 compares the models showing the highest load and the yield point. It further confirms the previous observation that the stacking (90°, 45°, -45°) experiences more load than the (0°, 45°, -45°) stacking and that a higher clearance% increases the strength of the L-joint. Furthermore, it shows that the increase in strength is highest at the 5% hole clearance, and the increase % is reduced as the hole clearance increases.

Table 1 Comparison between the effects of stacking and hole clearance

Hole Clearance	(90°, 45°, -45°) N/mm	(0°, 45°, -45°) N/mm	Increase %
5%	91.493	118.816	30%
10%	174.319	206.636	19%
15%	218.878	256.008	17%

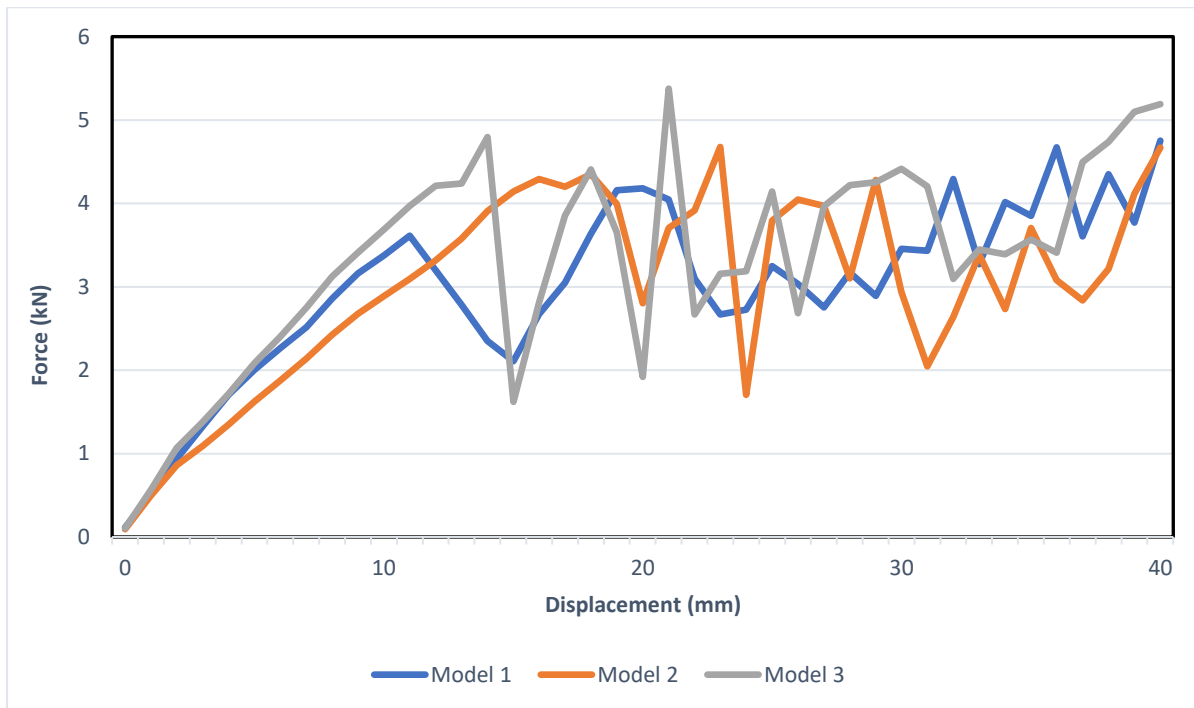


Figure 5 Results of L-joint models 1, 2 and 3

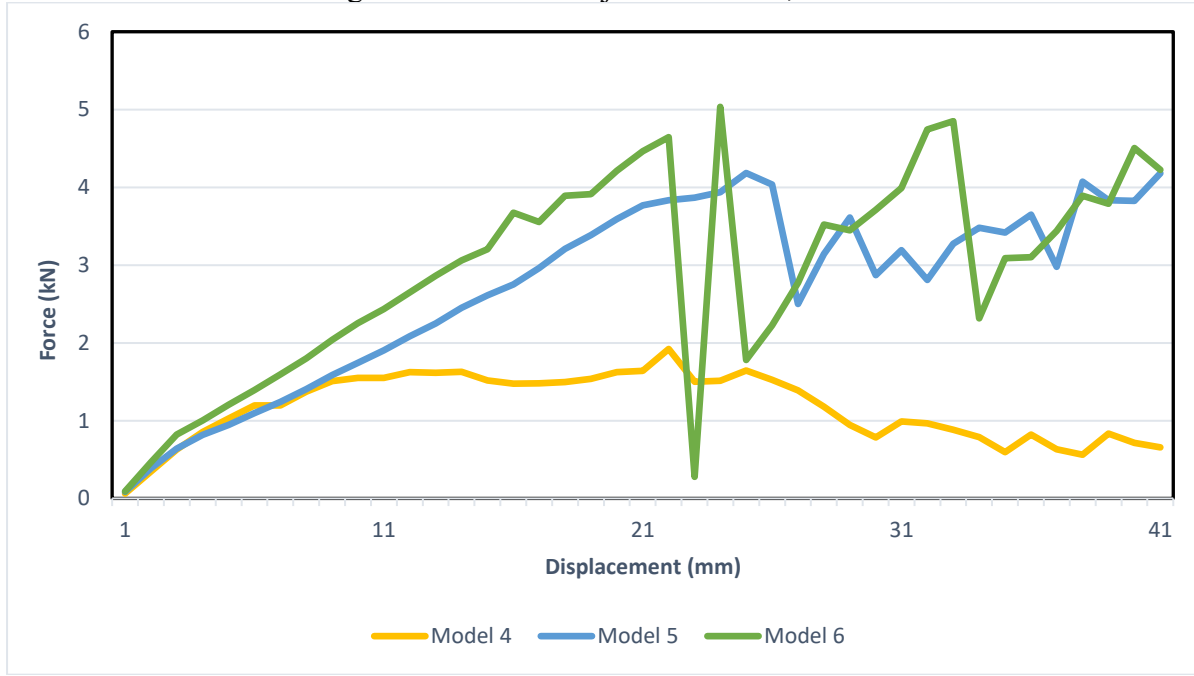


Figure 6 Results of L-joint models 4, 5, and 6

B. EFFECT ON THE MATRIX AND FIBER

Figures 7 to 9 show that the areas affected the most are around the hole, where there is contact between the washers and the ply, and at the curved area of the ply. Moreover, as shown in Figure 7, as the load progresses, the opposite ends start to straighten in the curved regions, causing the load effect to gradually shift toward the area surrounding the hole.

They also show that the failure of the fiber tension and compression is around the hole. However, the matrix tension and compression had a wider spread around the hole and on the curved area as well. The upper and lower layers experience compression in the area surrounding the bolt and tension in the curved area.

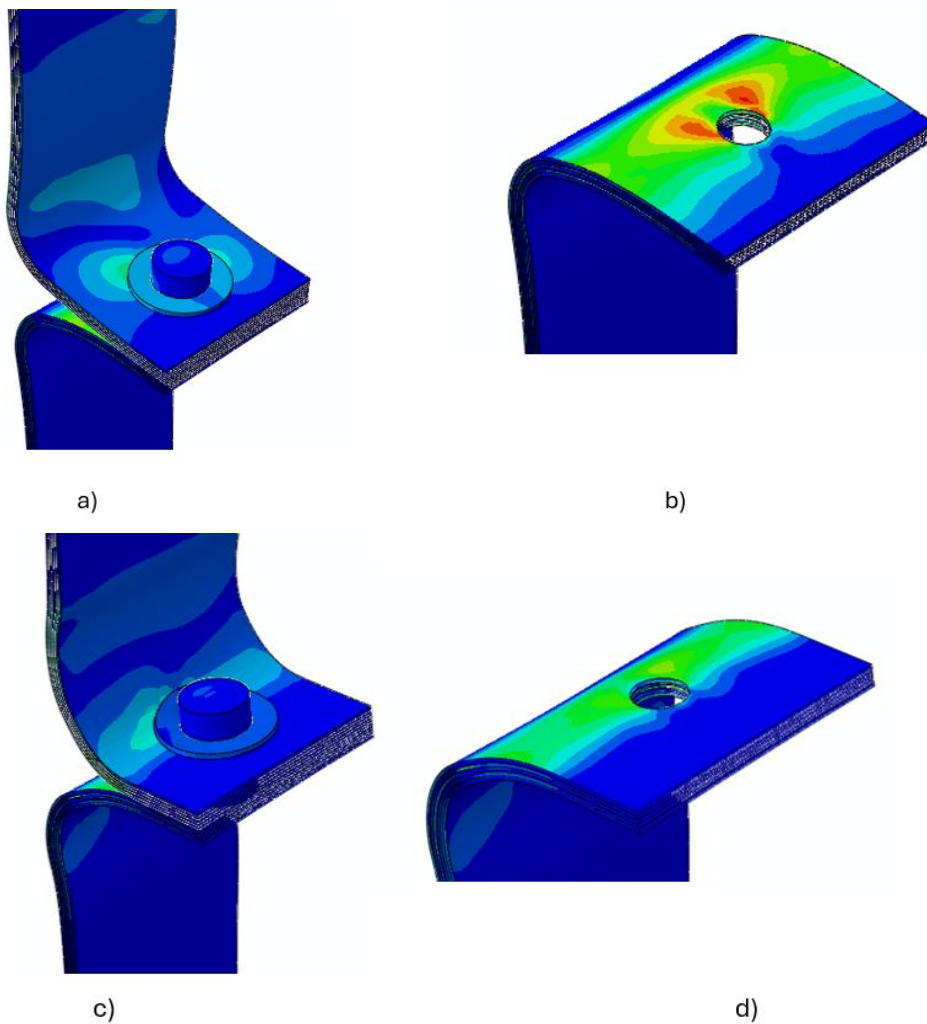


Figure 7 Stress distribution
a) Upper L-joints during elastic deformation
b) Lower L-joints during elastic deformation
c) Upper L-joints after elastic deformation
d) Lower L-joints after elastic deformation

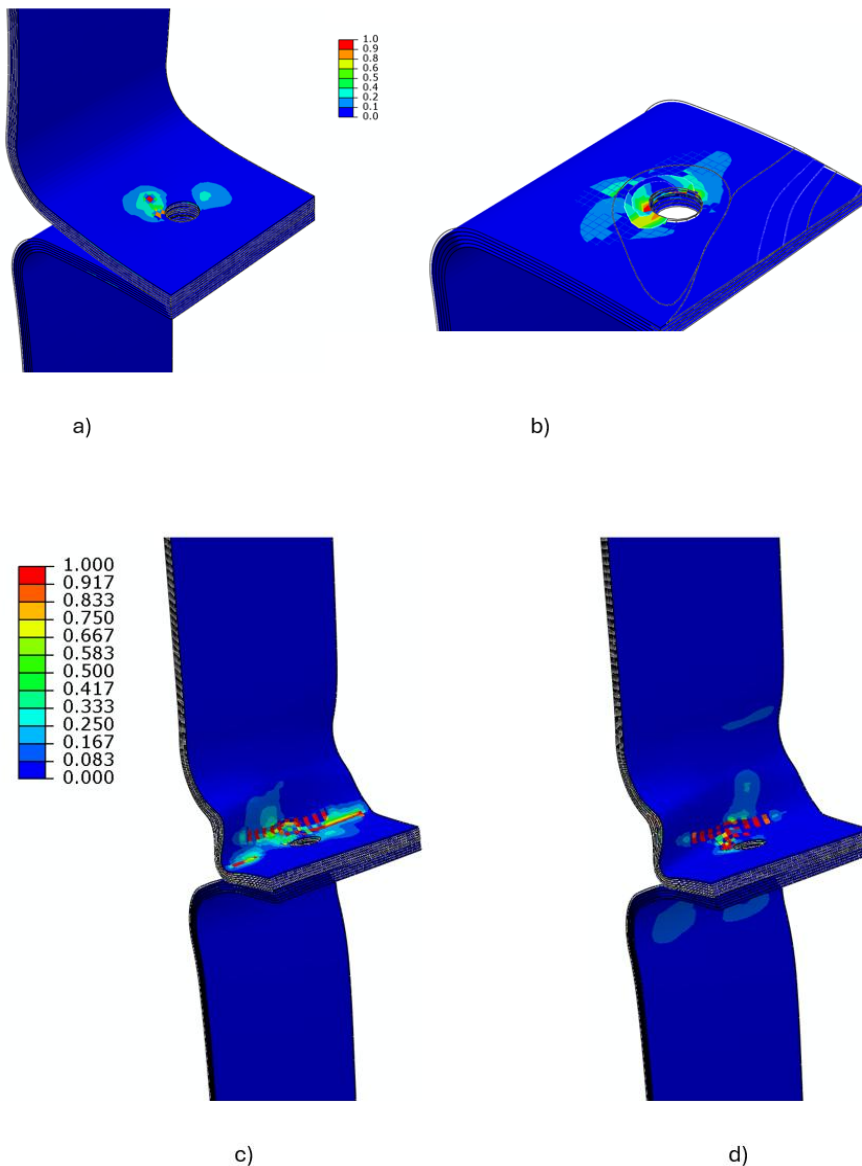


Figure 8 Hashin criteria a) Fiber compression during elastic deformation b) fiber tension during elastic deformation c) Fiber compression after elastic deformation d) fiber tension after elastic deformation

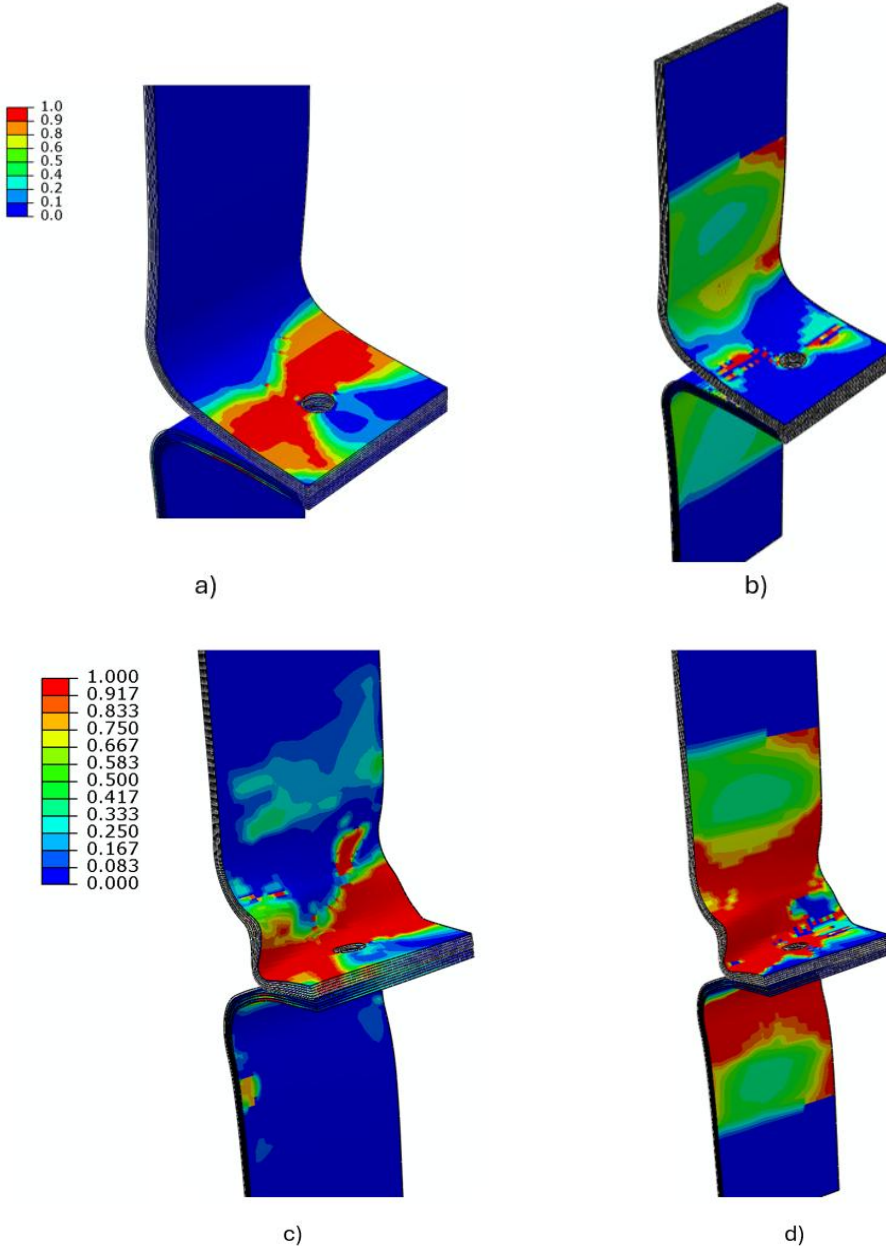


Figure 9 Hashin criteria a) Matrix compression during elastic deformation b) Matrix tension during elastic deformation c) Matrix compression after elastic deformation d) Matrix tension after elastic deformation

IV. CONCLUSION

After observing the results, the following was concluded:

- Stacking orientation has an effect on the strength of the L-joint, ply with $(0^\circ, 45^\circ, -45^\circ)$ can withstand higher loads than those of the $(90^\circ, 45^\circ, -45^\circ)$ up to 30%. However, the $(90^\circ, 45^\circ, -45^\circ)$ experience longer elastic deformation.
- Increasing the hole size relative to the bolt size also increases the L-joint strength, but the increase percentage is reduced as the size increases.
- Joints with 10% clearance experience more elastic behavior than the 5% and 15% clearance.
- The areas of the ply affected the most are around the hole and on the curved areas.
- The fiber experiences tension and compression around the hole, while the matrix has wider spread around the hole and curved areas.



V. THANKS

At the end of this research, we would like to sincerely thank:

- The British University in Egypt for providing necessary tools and funding for this research.

REFERENCES

- [1] Kaw, A. K. (2006). Mechanics of composite materials. Taylor & Francis.
- [2] Leon, M. S. H., Nomadas, S., Shahriar, M. S., & Dhar, N. R. (2025). Investigation of mechanical properties of natural fibers reinforced multilayered polymer matrix composites. <https://doi.org/10.1016/j.heliyon.2025.e44051>
- [3] Horsfall I, Hansen B, Carr D. Security of bolted joints during explosive loading. *Int J Veh Struct Syst* 2011;3(2).
- [4] Heimbs S, Schmeer S, Blaurock J, et al. Static and dynamic failure behaviour of bolted joints in carbon fibre composites. *Compos Part A Appl Sci Manuf* 2013;47: 91–101.
- [5] Brake MRW. A Reduced Iwan model that includes pinning for bolted joint mechanics. *Nonlinear Dyn* 2017;87(2):1335–49.
- [6] Zhang DM, Gao SQ, Niu SH, et al. Study on collision of threaded connection during impact. *Int J Impact Eng* 2017;106:133–45.
- [7] Gao S, Li J, Guo L, et al. Mechanical properties and low-temperature impact toughness of high-strength bolts after elevated temperatures. *J Build Eng* 2022;57: 104851.
- [8] Bickford, J. H. (2007). Introduction to the Design and Behavior of Bolted Joints, Fourth Edition. CRC Press.
- [9] M. Oppe and J. Knippers, "A consistent design concept for bolted connections in standardized GFRP-profiles", *Adv. FRP Compos. Civ. Eng. - Proc. 5th Int. Conf. FRP Compos. Civ. Eng. CICE 2010*, pp. 107–110, 2001.
- [10] Mahmoud, H. A. M. (2021). Analysis of composite bolted connections under out-of-plane loading (Master's thesis). Faculty of Engineering, Cairo University.
- [11] Cheng, X., Wang, S., Zhang, J., Huang, W., Cheng, Y., & Zhang, J. (2017). Effect of damage on failure mode of multi-bolt composite joints using failure envelope method. *Composite Structures*, 160, 8–15. <https://doi.org/10.1016/j.compstruct.2016.10.042>
- [12] Smith, M. "Abaqus/CAE User's Manual," Dassault Systèmes Inc. Provid. RI, USA, 2020
- [13] Z. Hashin and A. Rotem, "A Fatigue Failure Criterion for Fiber Reinforced Materials" *Journal of Composite Materials*, Vol. 7 (1973), pp. 448–464, doi: 10.1177/002199837300700404.